



# Thermal and mechanical properties of an epoxidized natural rubber composite containing a Li/Cr co-doped NiO-based filler

Bualan KHUMPAITOO<sup>1,\*</sup>, Songkot UTARA<sup>1,2</sup>, and Punyarat JANTACHUM<sup>1,2</sup>

<sup>1</sup>Division of Chemistry, Faculty of Science, Udon Thani Rajabhat University, 41000 Thailand

<sup>2</sup>Polymer and Material Research Groups, Division of Chemistry, Udon Thani Rajabhat University, 41000 Thailand

\*Corresponding author e-mail: bualan.kh@udru.ac.th

## Received date:

12 May 2018

## Accepted date:

17 June 2018

## Keywords:

Nickel oxide  
Rubber composites  
Thermal properties  
Mechanical properties

## Abstract

Li and Cr co-doped NiO-based (LCNO) filler was successfully synthesized by the sol-gel process using metal nitrate compounds as starting materials and citric acid as a crosslinking agent, followed calcination at a temperature of 1000°C for 3 h. Composites of Li and Cr co-doped NiO/epoxidized natural rubbers with 25 mol% epoxidation (abbreviated as LCNO/ENR-25) were prepared by mixing using a two-roll mill. The ENR-25 was blended with 0.5, 1, 2 and 3 phr (parts per hundred of rubber) of LCNO and the specimens were shaped at 160°C using compression molding. The LCNO/ENR-25 composites were characterized by thermogravimetric analysis (TGA), Fourier-transform infrared spectroscopy (FT-IR) and scanning electron microscopy (SEM). Additionally, a tensile tester was used to measure tensile strength, elongation at break and the modulus at 100% strain of the composites. The thermogravimetric analysis showed a slight increase in the decomposition temperature of the rubber composites with the addition of LCNO. The best dispersion of LCNO filled ENR-25 was observed with an LCNO loading of 3 phr. The incorporation of LCNO into ENR-25 resulted in an increase in the tensile strength and elongation at break, but decreased the modulus at 100% strain. The LCNO/ENR-25 composite with a content of 3 phr had the highest elongation at break (711%) and the highest tensile strength (18 MPa) compared to that of the ENR-25 vulcanizates (673% and 17 MPa, respectively), probably due to the better dispersion of LCNO in ENR-25.

## 1. Introduction

The desired characteristic of the materials with hybrid properties between the high dielectric constant and stiffness of ceramic materials and excellent mechanical strength, flexibility, formability, and robustness of polymer are much attractive for their potential impact in electronic devices such as integrated capacitors, antennas for mobile devices, sensors [1,2]. The composites with ceramic particles (0-D) dispersed in three-dimensionally connected polymer matrix (3D) are referred to as 0-3 connectivity [3]. The ceramic particles do not contact with each other, but the polymer phase is self-connected in all directions in the 0-3 connectivity. The 0-3 connectivity composites have been many reported such as lead zirconate titanate (PZT)/polyvinylidene fluoride (PVDF) [4], barium titanate (BT)/PVDF-TrFE [5], BaTiO<sub>3</sub>/natural rubber (NR) and PbTiO<sub>3</sub>/NR [1], BaTiO<sub>3</sub>-OH/NR [6,7], PZT/polyethylene and PZT/nylon57 [8], SiC/epoxidized natural rubber/NR [9], Li<sub>0.30</sub>Ti<sub>0.02</sub>Ni<sub>0.68</sub>O-carbon nanotube/epoxy resin [10] and Li<sub>0.30</sub>Cr<sub>0.10</sub>Ni<sub>0.60</sub>O/PVDF [11]. However, the combination of co-doped NiO-based ceramics with polymer in 0-3 connectivity composites has been little

reported. Interestingly, Li and Cr co-doped NiO-based ceramics have much attention from the researchers due to an observation of the very high dielectric constant. Recently, Li and Cr co-doped NiO-based (Li<sub>0.30</sub>Cr<sub>0.10</sub>Ni<sub>0.60</sub>O) ceramics are used as filler in PVDF matrix as previous our work [11]. These composites show the hydroxyl groups grafted onto the surface position of Li<sub>0.30</sub>Cr<sub>0.10</sub>Ni<sub>0.60</sub>O particles, which are as the polar molecules. Moreover, it is found that the high dielectric constant was weakly dependent on the wide frequency range, which suitable for capacitor applications. Natural rubber (NR) is the one most of the matrix because of its low-temperature flexibility, high elasticity, fatigue resistance, tearing resistance, low heat buildup and building tack [6]. However, NR is poor polar molecules. Thus, the NR modification by incorporation of polar functional groups such as epoxidized NR is used as a polymer matrix to prepare 0-3 connectivity composites. However, the addition of filling Li and Cr co-doped NiO-based ceramic in epoxidized NR matrix has never been reported so far. Therefore, the aim of this work was to prepare the composites of Li and Cr co-doped NiO-based filler particles in stoichiometry of Li<sub>0.30</sub>Cr<sub>0.10</sub>Ni<sub>0.60</sub>O with epoxidized natural rubbers with 25 mol% epoxidation

matrix (abbreviated as LCNO/ENR-25). In this process, the two roll-mill mixing method was chosen to prepare these composites. The advantages of this method are the high shear developed at mill nip, this breaks up agglomerates and drives incorporation of ingredient [12]. The deagglomeration and well-distribution and dispersion of the LCNO filler particles in the ENR-25 matrix that was suitable for making good composites could be expected. The addition of LCNO filler particles on thermal and mechanical properties of these composites was also investigated.

## 2. Materials and Experimental

### 2.1 Materials

In this research, ENR with 25 mol% epoxide (ENR-25) used as the matrix material was obtained by Muang Mai Guthrie Public Co., Ltd. Phuket, Thailand. Zinc oxide (white seal) and stearic acid used as activators were purchased from Global Chemical Co., Ltd. (Samutprakarn, Thailand) and Imperial Industry Chemical Co., Ltd. (Pathumtani, Thailand), respectively. Mercaptobenzothiazole (MBT) used as an accelerator was manufactured by Flexsys (Termoli, Italy). The sulfur used as a vulcanizing agent supplied by Ajax Chemical Co., Ltd. (Samutprakarn, Thailand). The starting materials  $\text{Ni}(\text{NO}_3)_2 \cdot 6\text{H}_2\text{O}$  (Ajax Fineman),  $\text{LiNO}_3$  (Himedia),  $\text{Cr}(\text{NO}_3)_3 \cdot 9\text{H}_2\text{O}$  (Himedia) and citric acid (V.S. Chem house) were selected to prepare  $\text{Li}_{0.30}\text{Cr}_{0.10}\text{Ni}_{0.60}\text{O}$  fillers. All the reagents were analytical grade.

### 2.2 Synthesis of $\text{Li}_{0.30}\text{Cr}_{0.10}\text{Ni}_{0.60}\text{O}$ (abbreviated as LCNO) fillers

The LCNO fillers were synthesized by the sol-gel process. A stoichiometric amount of  $\text{Ni}(\text{NO}_3)_2 \cdot 6\text{H}_2\text{O}$  and  $\text{LiNO}_3$  was dissolved in aqueous citric acid to get clearly green solution. After that stoichiometric proportion of  $\text{Cr}(\text{NO}_3)_3 \cdot 9\text{H}_2\text{O}$  was slowly added into the green solution and then refluxed for 2 h to get a sol-gel solution, followed by drying at  $250^\circ\text{C}$ . The dried gel was calcined at  $1000^\circ\text{C}$  for 3 h in air to obtain LCNO powder. The synthesis and characterization of LCNO fillers have also been reported in previously our work [11,13].

### 2.3 Synthesis of LCNO/ENR-25 composites

The formulation of LCNO/ENR-25 composites is shown in Table 1. The LCNO were used as fillers in this work, which was various the parts per hundred of rubber (phr) of 0, 0.5, 1, 2 and 3. Firstly, ENR-25 was done on the two-roll mill (ML-D150L350, Chareon Tut Co., Ltd., Thailand) according to ASTM D3184 for 3 min, followed by the LCNO fillers were continued mixing for 5 min. Then, zinc oxide and stearic acid were added and mixed for 3 min. MBT and sulfur were also added and mixed for 5 min. At the end of mixing, 10 end-roll passes were made before sheeting the compound off. The sheeted rubber compounds were kept at  $25^\circ\text{C}$  for 24 h in a closed container before vulcanizing. Rubber vulcanizates were prepared by compression molding at  $160^\circ\text{C}$  with an applied force 10 MPa in a hot press for 5 min.

**Table 1.** Formulation used to prepare LCNO/ENR-25 composites.

Ingredients	Quantity (part per hundred of rubber, phr)
ENR-25	100
LCNO	0, 0.5, 1, 2, 3
ZnO	6
Stearic acid	0.5
MBT	0.5
Sulfur	3.5

### 2.4 Characterization of LCNO/ENR-25 vulcanizates

The appearance of the functional groups of organic species in LCNO/ENR-25 rubber vulcanizates was investigated in the  $450\text{--}4000\text{ cm}^{-1}$  spectral range by Fourier transform infrared spectrometer (FT-IR) coupled to an attenuated total reflection (ATR) accessory with a diamond crystal, Perkin Elmer, Spectrum Two.

Thermal decomposition of the selected LCNO/ENR-25 rubber vulcanizates was examined by thermogravimetric analysis (TGA), Perkin Elmer, Pyris Diamond, heated up to  $950^\circ\text{C}$  with the heating rate of  $10^\circ\text{C}/\text{min}$  in nitrogen gas flow.

Morphology of the selected LCNO/ENR-25 rubber vulcanizates was observed using scanning electron microscope (SEM), Hitachi, S-3000N.

LCNO/ENR-25 rubber vulcanizates were measured the swelling ratio ( $Q$ ) by cutting into

20×20×2 mm<sup>3</sup> sized pieces and weighted using electronic balance. Then, the vulcanized specimens were immersed in 50 ml toluene at room temperature for 7 days. The swollen rubbers removed from the solvent and excess toluene was blotted with towel paper and weight accurately. The swelling ratio was calculated by the following equation [14].

$$Q = \frac{w_s - w_u}{w_u} \quad (1)$$

where  $w_u$  and  $w_s$  are the weights of the unswollen rubber and swollen rubber, respectively.

Hardness of LCNO/ENR-25 rubber vulcanizates was determined by a Shore A diameter (Frank GmbH, Hamburg, Germany), according to ASTM D2240. The six positions for each specimen were performed and calculated on an average value.

The dumb-bell shaped specimens were cut from the vulcanized sheets by following ASTM D412. Tensile properties of the specimens were measured by an Instron Universal Testing Machine (Model 3366) with a crosshead speed of 500 mm/min and an initial clamp separation 65 mm. The results from the tensile measurement were exhibited in term of the modulus, elongation at break and tensile strength.

### 3. Results and discussion

TGA curves of ENR-25 vulcanizate and the selected rubber composites of 1 phr LCNO/ENR-25 and 3 phr LCNO /ENR-25 are displayed in Figure 1 and found that TGA curves exhibited two major losses. The decomposition of an evaporation of relative volatile molecules occurred in the first step at temperature below 200°C [7]. Secondly, the large weight loss in the temperature range of 200-500°C, and there is almost no obvious weight loss above 520°C that could be ascribed to decomposition behavior of the epoxidized natural rubber [15]. In addition, the thermal degradation of ENR could be regarded as a two-step degradation [15-16]. In the first degradation step (Figure 1(b)), the lower temperatures of the rubber composites with LCNO loading of 1 phr and 3 phr of 370°C and 372°C, respectively, were observed in comparison with the ENR-25 vulcanizate (374°C). This result was probably due to shielding of ENR self-crosslinking by filler during vulcanization [16]. In Figure 1(c),

the second temperature degradation of ENR-25 vulcanizate and the rubber composites with LCNO contents of 1 phr and 3 phr were 450, 462 and 465°C, respectively. It is seen that the second temperature degradation increased with increasing LCNO content, indicating to the rubber composites more thermal stability than that of ENR-25 vulcanizate. The thermal temperature curves of the rubber composites were a little shifted to high temperatures as shown in the inset in Figure 1(c).

The FT-IR spectra of ENR-25 vulcanizate and all rubber composites with varying LCNO contents are given in Figure 2 and showed that the appearance of the characteristic bands of organic species corresponded to the epoxidized natural rubber [17], which were at 2955 cm<sup>-1</sup> (C-H stretching of CH<sub>3</sub>), 2854 cm<sup>-1</sup> (C-H symmetry stretching of CH<sub>2</sub>), 1666 cm<sup>-1</sup> (C=C stretching), 1486 cm<sup>-1</sup> (C-H bending of CH<sub>2</sub>), 1382 cm<sup>-1</sup> (C-H deformations of the carbon backbone), 1055 cm<sup>-1</sup> (C-O stretching of epoxide ring), 870 cm<sup>-1</sup> (C-O-C stretching of the partial ring opening of epoxide group) and 835 cm<sup>-1</sup> (C=CH wagging). Although, the M-O vibration band from LCNO fillers added to the rubber formulation were disappearance in FT-IR spectra due to the very low concentration and well-mixing process [6]. The O-H stretching vibration band of water or hydroxyl group present on the LCNO surfaces [11] were observed for all rubber composites. In Figure 2(a), it is seen that the intensity of hydroxyl group increased with increasing of LCNO loading up to 1 phr and then decreased. Moreover, the band of vibration at 1055 cm<sup>-1</sup> correspond to C-O stretching, as shown in Figure 2(b), led to increase of intensity and shifted to higher wavenumber after LCNO loading as 1 phr. These peak intensities might be ascribed to the polar functional groups in ENR interaction with the hydroxyl groups on LCNO surfaces, corresponding to the other result in carbon nanotube filled ENR [16].

The fracture surface morphology of the rubber composites containing different LCNO contents as 1 phr and 3 phr was observed by SEM technique in Figure 3. It can be seen that some portion of LCNO agglomerates in the micrograph of the composite loading LCNO content of 1 phr. Whereas, the rubber composite with LCNO content of 3 phr was better homogeneous dispersion in the rubber than that of 1 phr, resulting in enhancement of mechanical properties.

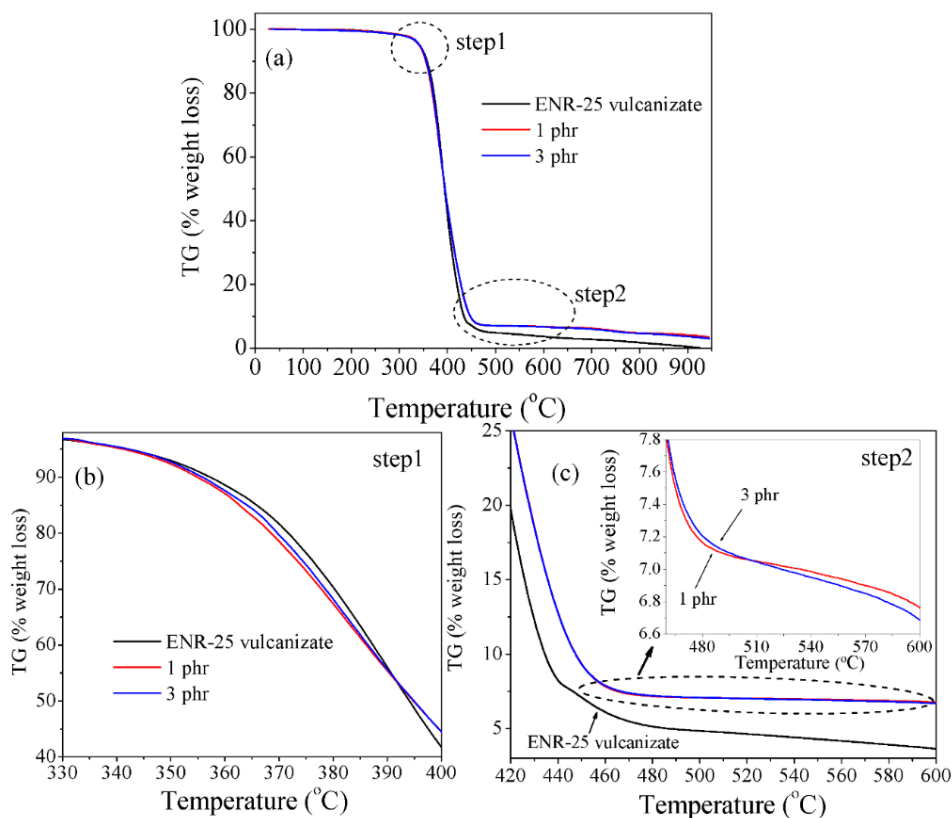


**Figure 1.** TGA curves of (a) ENR-25 vulcanizate and the selected rubber composites with various LCNO contents, the expand scale of temperature degradation of (b) the first step and (c) the second step, respectively.

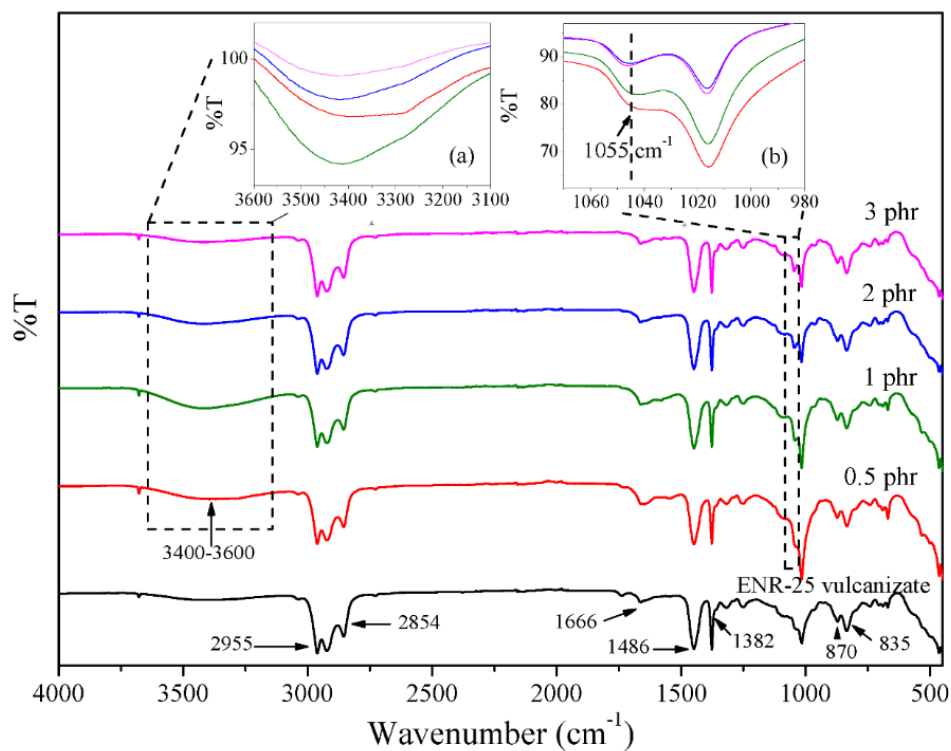


**Figure 2.** FT-IR spectra of ENR-25 vulcanizate and all rubber composites with varying LCNO contents.

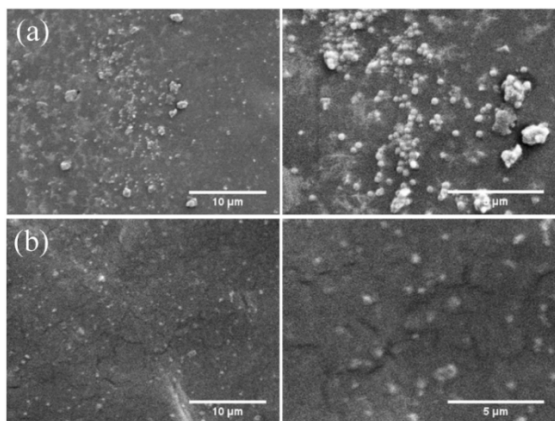


**Figure 3.** SEM micrographs with low (left) and high (right) magnifications of fracture surface of the selected rubber composites with various LCNO contents of (a) 1 phr and (b) 3 phr.

The swelling ratios of ENR-25 vulcanizate and the rubber composites with different LCNO filler contents were illustrated in Figure 4. The swelling ratio of ENR-25 vulcanizate was  $4.16 \pm 0.02$ . For the swelling ratios of the rubber composites with LCNO contents of 0.5, 1, 2 and 3 phr were  $4.04 \pm 0.01$ ,  $4.05 \pm 0.05$ ,  $4.05 \pm 0.01$  and  $3.92 \pm 0.02$ , respectively, which were not significantly change with LCNO content. It can be seen that the swelling ratios were slightly decreased with the addition LCNO filler into the ENR-25, corresponding to the other report [18]. This could be ascribed to the improvement of filler-rubber interaction.

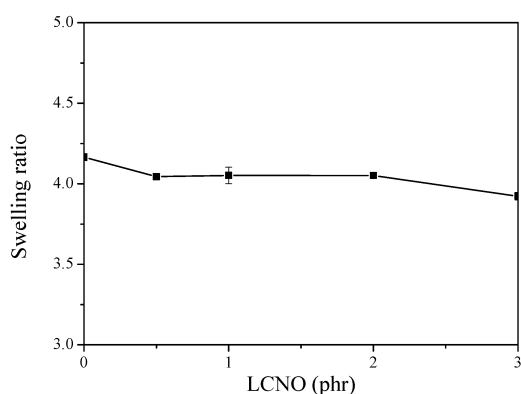


**Figure 4.** Swelling ratio of ENR-25 vulcanizate and the rubber composites with the different addition of LCNO filler.

The hardness values and 100% modulus of all vulcanizate samples are shown in Figures 5(a) and (b), respectively. It can be seen that the both values of hardness values and 100% modulus trended to increase as a LCNO filler increased up to 2 phr and

then decreased, whereas the elongation at break (Figure 5(c)) exhibited the opposite trend. This result related to the lower the degree of swelling or higher cross-linking density, which could be explained by homogeneous dispersion in these samples from SEM images and the improvement of filler-rubber interaction [18-19]. Among these composites, the loading LCNO content of 3 phr filled with ENR-25 had the highest elongation at break of 711%. Figure 5(d) showed the tensile strength of all rubber composites and found that the tensile strength of the rubber composites with LCNO loading lower than 1 phr were decreased, due to the low chain interaction and high agglomerated system after the vulcanization process [7]. Whereas, the LCNO/ENR-25 composites with addition LCNO contents from 2 phr to 3 phr had the increase of tensile strength. This might be explained by the higher interaction between LCNO and rubber matrix because of the presence of the better dispersion of LCNO filled with ENR-25 matrix as observed in SEM result, correlating to the other reports [7,18]. The LCNO/ENR-25 composite with LCNO content of 3 phr showed the highest tensile strength and the highest elongation at break with good dispersion in comparison with the other rubber composites.

According to the result, the fabricated rubber composites with various LCNO contents were prepared by the two roll-mill mixing and followed by hot pressing at 160°C to obtain the vulcanizate samples. The result from all FT-IR spectra was not significantly different the characteristic bands of ENR-25 matrix and the characteristic vibration bands of M-O stretching of LCNO filler were not observed in FT-IR spectra because of the very low concentration and well-mixing process, in agreement with the other work in the addition of 0-0.5 wt% BaTiO<sub>3</sub> loading into NR [6]. However, the intensities of O-H and C-O stretching were slightly change might due to occur the interaction between ENR-25 and LCNO filler. The microstructure of rubber composites showed some agglomeration in the LCNO loading of 1 phr, which probably resulting from the electrostatic interaction as found in the BaTiO<sub>3</sub> filled with natural rubber [7]. The result of electrostatic interaction among LCNO and the other additive such as ZnO also appeared in the rubber formulation. The repulsion forces occurred interfacial interaction between the particles, resulting in the agglomeration. For the addition of LCNO content as 3 phr, the better

homogeneous dispersion in the ENR-25 matrix was observed. This might be attributed to the higher chemical interaction between LCNO and ENR matrix. It has been reported that the surface composition of co-doped NiO-based consisted of hydroxyl groups and metal oxides [10-11]. Moreover, the hydroxyl groups in these composite samples were obtained in FT-IR spectra. Therefore, the formation of hydrogen bonding between hydroxyl groups and metal oxides with epoxide groups in ENR molecules probably occurred. This is a reason led to enhance the thermal properties and mechanical properties. As expected, the influence of LCNO filler was to improve in thermal and mechanical properties. In the thermal analysis result, TGA curves of the rubber composites with the addition of LCNO filler showed a slight increase in the decomposition temperature. This result might be attributed by the effect of confinement of chain movement caused by an increase in the cross-linking degree [7]. Additionally reason to explain the increase of the thermal stability, the interaction between hydroxyl groups grafted onto surface of LCNO filler and the epoxide group in ENR-25 matrix was probably pronounced, leading to an increase stability of rubber polymer chains against thermal degradation [16,20]. The best of LCNO/ENR-25 composite with containing LCNO content of 3 phr exhibited higher mechanical

properties including harness value, elongation at break and tensile strength than those of ENR-25 vulcanizate. This was probably due to the incorporation of the polar surface hydroxylated LCNO filler with good distribution interacted with the polar functional group as epoxide groups in the ENR molecules caused high filler-rubber interaction. This explanation was supported by the higher chemical interaction and the better dispersion of LCNO in the ENR-25 rubber as found in SEM result, resulting in enhancement the mechanical properties. The changes in swelling ratio and mechanical properties were too small in this work might due to the very low concentration of LCNO filler added to the rubber formulation. However, the best result of this work was agreed well with the other reports which in the tensile strength and elongation at break of LCNO/ENR-25 composite with containing LCNO content of 3 phr were 18 MPa and 711%, which were nearly close to the other fillers in ENR matrix [1,9]. Based on the LCNO filler had the very high dielectric constant with a weak temperature and frequency dependence [13]. Interestingly, the dielectric and electrical properties of ENR matrix with high dielectric constant as LCNO filler should be also measured in the further investigation. This aspect would be checking the dielectric tendency behavior for making the flexible capacitor applications.

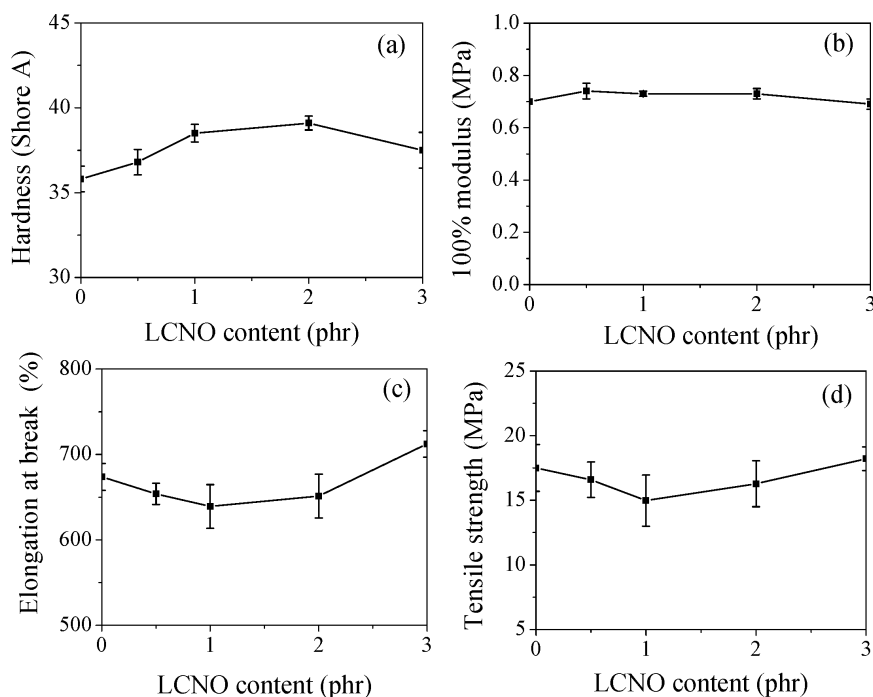


**Figure 5.** Mechanical properties of LCNO/ENR-25 composites with various LCNO contents showing (a) hardness, (b) 100% modulus, (c) % elongation at break and (d) tensile strength.

#### 4. Conclusions

The epoxidized natural rubber composites containing  $\text{Li}_{0.30}\text{Cr}_{0.10}\text{Ni}_{0.60}\text{O}$  filler prepared by the two roll-mill mixing showed the increase of the thermal properties and mechanical properties, probably due to the higher chemical interaction and the better dispersion of fillers in the epoxidized natural rubber. The composite loading  $\text{Li}_{0.30}\text{Cr}_{0.10}\text{Ni}_{0.60}\text{O}$  of 3 phr had the good morphology with the highest tensile strength and elongation at break.

#### 5. Acknowledgements

This work would like to thank the Division of Chemistry, Faculty of Science, Udon Thani Rajabhat University for its research support and Rubber Technology Research Centre (RTEC), Faculty of Science, Mahidol University for providing the tensile properties measurement facility.

#### References

- [1] S. Salaeh, N. Muensit, P. Bomlai, and C. Nakason, "Ceramic/natural rubber composites: influence types of rubber and ceramic materials on curing, mechanical, morphological, and dielectric properties," *Journal of Materials Science*, vol. 46, pp. 1723-1731, 2011.
- [2] A. A. Al-Ghamdi, O. A. Al-Hartomy, F. R. Al-Solamy, N. Dihovsky, M. Mihaylov, P. Malinova, and N. Atanasov, "Natural rubber based composites comprising different types of carbon-silica hybrid fillers. Comparative study on their electric, dielectric and microwave properties, and possible applications," *Materials Sciences and Applications*, vol. 7, pp. 295-306, 2016.
- [3] R. E. Newnham, D. P. Skinner, and L. E. Cross, "Connectivity and piezoelectric-pyroelectric composites," *Materials Research Bulletin*, vol. 13, pp. 525-536, 1978.
- [4] B. Hilczer, J. Kulek, E. Markiewicz, M. Kosec, and B. Malič, "Dielectric relaxation in ferroelectric PZT-PVDF nanocomposites," *Journal of Non-Crystalline Solids*, vol. 305, pp. 167-173, 2002.
- [5] J. Li, J. Claude, L. E. Norena-Franco, S. I. Seok, and Q. Wang, "Electrical energy storage in ferroelectric polymer nanocomposites containing surface-functionalized  $\text{BaTiO}_3$  nanoparticles," *Chemistry of Materials*, vol. 20, pp. 6304-6306, 2008.
- [6] N. González, M. A. Custal, S. Lalaouna, J.-R. Riba, and E. Armelin, "Improvement of dielectric properties of natural rubber by adding perovskite nanoparticles," *European Polymer Journal*, vol. 75, pp. 210-222, 2016.
- [7] N. González, M. A. Custal, G. N. Tomara, G. C. Psarras, J.-R. Riba, and E. Armelin, "Dielectric response of vulcanized natural rubber containing  $\text{BaTiO}_3$  filler: The role of particle functionalization," *European Polymer Journal*, vol. 97, pp. 57-67, 2017.
- [8] W. Supmak, A. Petchsuk, and A. Thanaboonsombut, "Influence of ceramic particle sizes on electrical properties of lead zirconate titanate (PZT)/nylon57 composites," *Journal of Metals, Materials and Minerals*, vol. 18, pp. 147-151, 2008.
- [9] S. Utara, P. Jantachum, and B. Sukkaneewat, "Effect of surface modification of silicon carbide nanoparticles on the properties of nanocomposites based on epoxidized natural rubber/natural rubber blends," *Journal of Applied Polymer Science*, vol. 134, pp. 45289, 2017.
- [10] Y. Shen, G. Liang, L. Yuan, Z. Qiang, and A. Gu, "Unique  $\text{Li}_{0.3}\text{Ti}_{0.02}\text{Ni}_{0.68}\text{O}$ -carbon nanotube hybrids: Synthesis and their epoxy resin composites with remarkably higher dielectric constant and lower dielectric loss," *Journal of Alloys and Compounds*, vol. 602, pp. 16-25, 2014.
- [11] B. Khumpaitool, and S. Utara, "Preparation and characterization of  $\text{Li}_{0.30}\text{Cr}_{0.10}\text{Ni}_{0.60}\text{O}$ /polyvinylidene fluoride composites with high dielectric constants," *Ceramics International*, vol. 43, pp. S274-S279, 2017.
- [12] S. Shokeen, "A review on rubber compound mixing in Banbury mixer at time industries," *International Journal of Innovative Research in Technology*, vol. 2, pp. 232-236, 2015.
- [13] J. Khemprasit, and B. Khumpaitool, "Influence of Cr doping on structure and dielectric properties of  $\text{Li}_x\text{Cr}_y\text{Ni}_{1-x-y}\text{O}$  ceramics," *Ceramics International*, vol. 41, pp. 663-669, 2015.
- [14] N. Rattanasom, T. Saowapark, and C. Deeprasertkul, "Reinforcement of natural

- rubber with silica/carbon black hybrid filler,” *Polymer Testing*, vol. 26, pp. 369-377, 2007.
- [15] C. He, Y. Wang, Y. Luo, L. Kong, and Z. Peng, “Thermal degradation kinetics and mechanism of epoxidized natural rubber,” *Journal of Polymer Engineering*, vol. 33, pp. 331-335, 2013.
- [16] A. Krainoi, C. Kummerlöwe, Y. Nakaramontri, N. Vennemann, S. Pichaiyut, S. Wisunthorn, and C. Nakason, “Influence of critical carbon nanotube loading on mechanical and electrical properties of epoxidized natural rubber nanocomposites,” *Polymer Testing*, vol. 66, pp. 122-136, 2018.
- [17] W. A. K. Mahmood, M. M. Rahman Khan, and M. H. Azarian, “Sol-gel synthesis and morphology, thermal and optical properties of epoxidized natural rubber/zirconia hybrid films,” *Journal of Non-Crystalline Solids*, vol. 378, pp. 152-157, 2013.
- [18] S. Prasertsri, and N. Rattanasom, “Mechanical and damping properties of silica/natural rubber composites prepared from latex system,” *Polymer Testing*, vol. 30, pp. 515-526, 2011.
- [19] P. Boochathum, and N. Rongtongaram, “Influence of chloroacetate group on physical properties of natural rubber and its interaction with fillers,” *Journal of Applied Polymer Science*, vol. 133, pp. 43076, 2016.
- [20] S. F. Mendes, C. M. Costa, C. Caparros, V. Sencadas, and S. Lanceros-Méndez, “Effect of filler size and concentration on the structure and properties of poly(vinylidene fluoride)/BaTiO<sub>3</sub> nanocomposites,” *Journal of Materials Science*, vol. 47, pp. 1378-1388, 2012.